Towards Understanding Formation and Stability of Cyclodextrin Inclusion Complexes: Computation and Visualization of their Molecular Lipophilicity Patterns[1]

Frieder W. Lichtenthaler and
Stefan Immel, Darmstadt (Germany)

Five cyclodextrin inclusion complexes – typical examples for their solid state as well as exemplary "frozen molecular images" of their status in solution – were subjected to a molecular modelling study comprising the computer-assisted generation of the molecular lipophilicity patterns (MLP's), i.e. the *p*-iodoaniline inclusion into α-CD, the complexes of β-CD with 1,4-butanediol, adamantane-1-carboxylic acid, and adamantane-1-methanol, and the unique 12-crown-4 ether inclusion compound of γ-CD. Based on their solid state structures, the "solvent-accessible" contact surfaces were generated by the MOLCAD program. Calculation and color-coded projection of the MLP's onto these surfaces easily allows to locate the hydrophobic and hydrophilic surface regions of CD-host and guest alike. Their detailed analysis revealed a far-reaching, mostly complete conformity between the hydrophobic surface areas of the guest and the hydrophobic domains in the CD cavity. This striking tendency to optimize the reciprocal concurrence of lipophilic as well as hydrophilic domains at the guest-host-interface may accordingly be concluded to be an important, if not the decisive element in orienting the guest into the cavity and in determining the stability of the complex, particularly in cases where the guest is devoid of polar groups; if these are present, dipole-dipole alignments and the need for their solvation may diminish the importance of hydrophobic attractions for orienting and stabilizing the guest in the CD cavity.

Zum Verständnis der Bildung und Stabilität von Cyclodextrin – Einschlußverbindungen: Berechnung und Visualisation ihrer Lipophilie-Profile. Fünf Cyclodextrin-Einschlußverbindungen – typische Beispiele für ihren Zustand in fester Form, aber auch exemplarisch als „eingefrorene molekulare Bilder" ihres Zustandes in Lösung – wurden einer Molecular-Modelling-Studie unterworfen, und zwar: der *p*-Jodanilin-Einschluß in α-CD, die β-CD-Komplexe von 1,4-Butandiol, von Adamantan-1-carbonsäure und Adamantan-1-methanol, sowie der 12-Krone-4 Ether-Komplex von γ-CD. Ausgehend von den jeweiligen Röntgenstrukturen wurde mittels des MOLCAD Programms die für ein Lösungsmittel (Wasser) zugängliche Kontaktoberfläche generiert, und darauf dann, in Farbkodierung, die entsprechenden molekularen Lipophilie-Profile (MLP's) abgebildet, wodurch die hydrophoben und hydrophilen Oberflächenregionen von Gast und CD-Wirt klar lokalisierbar sind. ihre detaillierte Analyse offenbarte eine weitgehende, meist sogar vollständige Komplementarität zwischen hydrophoben Oberflächenzonen des Gastes und hydrophoben Bereichen des CD-Hohlraums. Diese eindrucksvolle Tendenz, ein optimales gegenseitiges Zusammenlagern lipophiler und hydrophiler Bereiche von Gast und Wirt zu verwirklichen, läßt darauf schließen, daß hydrophobe Wechselwirkungen ein wichtiger, wenn nicht entscheidender Faktor sind für die Orientierung des Gasts im Hohlraum und für die Stabilität des Komplexes – insbesondere dann, wenn der Gast keine ausgesprochen polare Gruppen trägt; sind solche vorhanden, kann die Notwendigkeit zur Ausrichtung von Dipolen und zur Solvatisierung der polaren Gruppen die Dominanz hydrophober Effekte deutlich vermindern.

1 Introduction

The most characteristic physical property of the cyclodextrins is their promiscuous behavior in forming complexes with a variety of organic and inorganic compounds by incorporating them into their hydrophobic cavities – in the solid state as well as in solution [2–4]. This has led to their exploitation for various purposes: in medicinal applications for providing pharmaceuticals with increased bioavailability [5], in chromatography for separation of enantiomers [6, 7], in catalysis [2, 8], in asymmetric reactions [9], as models for artificial enzymes [10], or even for the selective removal of cholesterol from egg yolk [11].

The bulk of X-ray [12], NMR [13], and computational [14–18] evidence available for cyclodextrins and their inclusion compounds, most notably a recent statistical analysis of the alltogether 100 solid state structures available [19], provide ample documentation that the CDs are flexible hosts which can adapt – within the limits of their annuli – to the topologies of the guests embedded into their cavities. Accordingly, the overall process of inclusion complex formation is best visualized to occur via an "induced fit" mechanism [20], rather than being symbolized by the overly rigid lock-and-key analogy [21].

Aside of the obvious requirement that the guest must fit into the cavity, even if only partially, various other effects have been adduced to be the actual driving forces governing the host-guest complexation [4], e.g. polar interactions, dipole-dipole alignments, entropic and enthalpic factors associated with solvation changes in the host and the guest – and, not the least – *hydrophobic interactions*. Although the latter may be a major factor in the formation of the complex and in securing its stability, it is exceedingly difficult to quantitatively separate these hydrophobic effects [22] from the variety of other binding interactions.

Recently, we have been able to demonstrate that the molecular lipophilicity patterns (MLP's) of sucrose [23, 24], of non-carbohydrate sweeteners [23], or cyclodextrins [19, 24–26], of non-glucose oligosaccharides [26] as well as of the amylose portion of starch [24] are a proper means to portrary their respective hydrophobic topographies. In fact, these MLP's generated by *Brickmann's* MOLCAD program [27] and mapped onto the respective contact surfaces [28] in color-coded form [29, 30], provided for the first time a lucid picture of the hydrophobic and hydrophilic surface regions – entities that are as yet quite elusive to exact experimental characterization.

It was obvious to extend our studies to the potentially intriguing interplay of hydrophobic interactions between guest and host in complexes of cyclodextrins. Accordingly, we report on the MLP profiles of representative inclusion compounds of α-CD, β-CD, and γ-CD, probing in how far the formation and stability of the complexes can be related to the hydrophobic characteristics of both, the host and the guest, respectively.

2 Results and Discussion

Although the gross orientation of the guest in the cyclodextrin cavity must not necessarily be the same in the solid state and in solution, there is ample evidence that this, in fact, is the case. For the α-CD *p*-nitrophenol complex, for example, this has been unequivocally proved [31, 32], and this also holds for the *m*-nitrophenol inclusion compound [32b, 33], since a report to the opposite [32a] was shown to be invalid by NOE experiments [32b]. So we feel justified to probe the relevance of the MLP's of CD-inclusion compounds on the basis of their solid state geometries, and, accordingly, have selected from the vast number of X-ray structures [12] – somewhat arbitrarily, for sure – one complex each of α-CD and γ-CD, and three β-CD inclusions, as representative examples.

2.1 The α-cyclodextrin – *p*-iodoaniline complex

The crystal and molecular structure of the α-CD *p*-iodoaniline trihydrate [34] is shown in Figure 1 (top entry) in a ball-and-stick model form, around which the contact surfaces of the guest and the host are superimposed in dotted form, signifying how far water molecules can approach. The *p*-iodoaniline guest is deeply buried in the α-CD cavity with the iodine atom pointing towards the primary 6-OH grous, while the amino group sticks out on the wide rim aperture without being hydrogen-bonded to the host. All glucose residues are uniformly in the $^4C_1$ conformation, and are canted with their primary hydroxyl groups towards the center of the molecule with tilt angles τ between 91–106° [35]. The macrocycle as such is essentially planar, since puckering deviations were in the 0.08Å range only. The cramming of the phenyl ring into the α-CD leads to a pronounced elliptical distortion of the macrocyclic perimeter with diagonal O_1-O_1-distances varying between 8.15 and 8.85Å. Thus, the tight steric fit of the guest inside the cavity – most lucidly apparent from the cross-section plots in Figure 1 (center and bottom entries) – is clearly due to the fact that the macrocyclic host has adjusted its geometry to the topology of the guest during complex formation, a process best envisaged to occur via an induced-fit-mechanism [20] rather than by the notion of lock-and-key [21], being is too rigid a system as to account for adaptation.

In Figure 2, the usual color-code (blue: most hydrophilic, yellow: most hydrophobic molecular surface areas) was applied to visualize the molecular lipophilicity patterns (MLP's) [29] generated by the MOLCAD-program [27]. Thereby, different modes of scaling were used: in the left entries of Figure 2, the color-scale was adapted to each molecule individually to illustrate the close spatial relationship of hydrophilic and hydrophobic surface regions of guest and host molecule ("private scaling"). The second scale ("absolute scaling", right entries in Figure 2) was chosen to demonstrate the entirely different hydrophobicities of guest and host in absolute terms, as *p*-iodoaniline is much more hydrophobic than α-CD. This mode again reflects the hydrophobic effect to substantially contribute to the driving force for the formation of the inclusion complex by diminishing the interface area between solvent and the aromatic ring with its iodine atom. Most notable from the individually scaled models – in particular from the side-view models (Fig. 2, bottom) where the surface has been partially sliced – is the excellent conformity of the most hydrophilic and the most hydrophobic surface regions on the guest-host interface: the iodine atom is located at the smaller torus opening (6-CH_2OH side), where the α-CD has its most hydrophobic cavity regions *a priori* [19]; correspondingly the amino function protrudes from the hydrophilic torus rim (secondary hydroxyl side) of the cyclodextrin ring.

The mutual host-guest conformity of hydrophilic and hydrohpobic surface areas is surmised to be similarly realized in the majority of other α-CD inclusion compounds, for example, in its complexes with benzaldehyde [36a], *p*-iodophenol [36b], *p*-nitrophenol [31], 1-phenylethanol [36c], sodium benzenesulfonate [36d], and sodium 1-propanesulfonate [36e]: invariably, the guest, when imbedded in the cavity, has its hydrophobic protions directed towards the hydrophobic primary hydroxyl side of the torus.

The correlation of the hydrophobic features of CD-host and guest may be outbalanced though by hydrogen bonding effects, particularly with small guests such as N,N-dimethylformamide [37], 2-pyrollidone [37] and 3-iodopropionic acid [38] which are not able to fill the cavity towards a reasonably close fit. In the latter case, for example, the iodine is located at

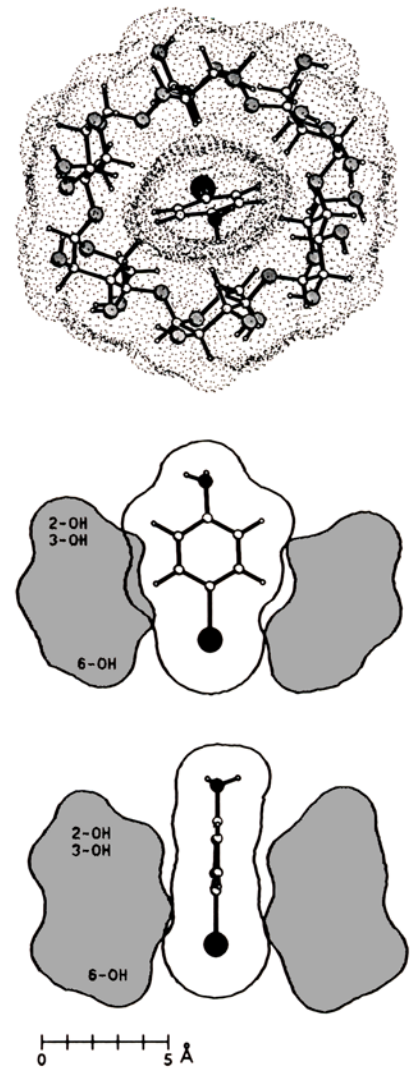

Figure 1. Topology of the α-CD *p*-iodoaniline trihydrate inclusion complex as derived from solid state structure [34b], with the three water molecules located at the CD-outside left off for clarity. *Top:* Contact surfaces in dotted form with ball-and-stick model insert, viewed from the wider opening (2-OH and 3-OH side) of the truncated cone; oxygen, nitrogen, and iodine atoms are shaded. – *Center* and *bottom:* Side-view surface cross-sections through the complex, perpendicular and parallel to the phenyl ring of the guest molecule. Aside the nearly perfect steric fit, the elliptical distortion of the CD macrocycle, matching the flact disc-type shape of the phenyl ring, becomes evident.

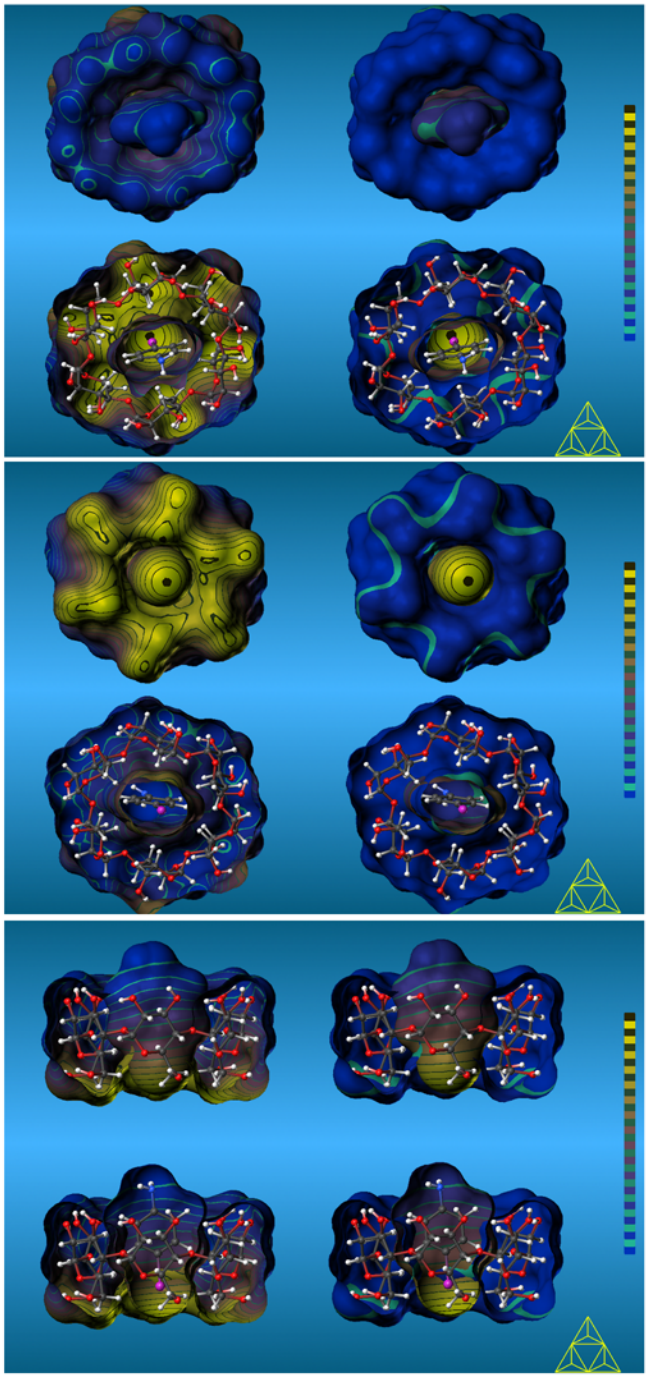

Figure 2. The molecular lipophilicity pattern (MLP) of the α-CD *p*-iodoaniline trihydrate inclusion complex [34b] in a two-color code, blue corresponding to hydrophilic surface areas, yellow-brown to the hydrophobic ones. Their calculation by the MOLCAD program [27] was done separately for guest and host, followed by subsequent reassembly to the complex. In the left-side images, the two-color code was adapted to the MLP range of guest and host separately ("private mapping"), revealing the nearly perfect correspondence between most hydrophilic and most hydrophobic surface regions (in relative terms). The *top* picture shows the inclusion complex in the same orientation as in Figure 1, i.e. the wide opened aperture (2-OH/3-OH side) of the cyclodextrin facing the viewer. To facilitate visualization, front-side-opened surface representations with ball-and-stick models inserted are provided underneath the closed solid-surface models, iodine being represented by a violet ball. The center entry shows the back-side of the inclusion complex with the 6-CH_2OH side directed towards the front. The *bottom* image displays side-view models with two different depths of surface slices through the CD torus "standing" on its primary hydroxyl side with secondary hydroxyls pointing upwards. The images presented at the right-side column result from adaptation of the color code to the absolute range of MLP values (in arbitrary units) for the complex as such, signifying the 2-OH/3-OH face of the β-CD host and the amino group-bearing portion of the *p*-iodoaniline guest to be the most hydrophilic surface regions (top right entry). The opposite side of the complex (center right) reveals the most hydrophobic area to be the iodine atom of the guest, with the 6-CH_2OH face still being distinctly hydrophilic. These guest-host inter-relationships are most vividly symbolized by the cross cuts (bottom entries, right), sustaining the notion that the relative distribution of hydrophobicity at the interface of both surfaces determines the orientation of the guest in the cavity.

the secondary hydroxyl side of the cavity, while the carboxyl group, at the other, forms a hydrogen bond to a secondary hydroxyl of the next α-CD. However, if this hydrogen bond interaction is blocked, as, for example, ina 2-*O*-,6-*O*-dimethylated α-CD, orientation of the 3-iodopropionic acid is reversed the iodine being located at the 6-CH_2OMe side [39]. This appears to be clear evidence, that the urge to match hydrophobic regions are by no means the only forces operating in orienting the guest into or within the cavity. Dipole-dipole interactions and hydrogen bonding with the suitable groups that may even involve water molecules, play a crucial role, as will become more apparent in a variety of β-CD inclusions.

2.2 The β-cyclodextrin — butanediol-(1,4)-complex

Elongated chain-type molecuels with hydrohilic head groups will tend to hide their more hydrophobic center parts form interaction with the solvent by threading into the cavity of the CD's. An illustrative example in this regard is the solid state structure of the β-CD 1,4-butanediol $\cdot$ 6.25H_2O inclusion complex [40], in which in addition to the guest ~1.25 water are enclosed in the cavity. In the complex, the CD unit itself is almost regularly round-shaped with glucose tilt angles [35] around $\tau \approx 110$ (10)° and glycosidic O_1-$O_{1'}$-distances diagonally across the CD-ring ranging between 9.34–10.17Å; the macrocycle is only slightly puckered, deviations from planarity (based on the atomic displacements of the seven intersaccharidic oxygens from a least-square best-fit) being around 0.19(8) Å.

The hydroxyl groups of the 1,4-butanediol are located at each end of the tonis and form hydrogen bonds with neighboring β-CDs and water [40]. Since the cavity is much larger than the *van der Waals* diameter of the guest, it vibrates extensively in its CD cage. As the atomic resolution of the structure determination is insufficient to differentiate between various disordered butanediol conformations, only the mean atomic positions of the guest could be established. By consequence, thermal averaging leads to a virtual covalent conformation of the chain, which in terms of bond lengths, angles, and torsions does not represent a real energy minimum conformation. The terminal butanediol oxygens are involved in smaller thermal motions than the carbon atoms are, indicating that hydrogen bonding interactions with adjacent β-CD molecules hold certain chain conformations in fixed positions.

Fortunately, for such simple molecules as 1,4-butanediol, the visualization of MLP maps on the corresponding molecular surfaces is almost independent from the exact conformation as long as the proper atomic hydrophobicity parameters are taken into consideration. The two hydroxyl groups repre-

sent the highly hydrophilic head groups, separated by an extended hydrophobic spacer, as is particularlly evident from the MLP profiles of the complex (Figure 4), the slightly inclined guest has its terminal polar OH groups placed at either rim of the torus with the unpolar aliphatic chain masked in the β-CD cavity.

In the light of this scenario, and the reflection that the solid state structure situation depicted in Figure 4 may be considered to be at least a "snapshot image" of its solution state, the guest-host conformity of hydrophobic and hydrophilic surface regions again becomes clearly evident. Particularly, the side-view models (Figure 4, bottom) illustrate lucidly the apolar environment provided by the β-CD cavity, and its function to hide the tetramethylene unit, thereby diminishing the corresponding solute-solvent interface in (aqueous) solution. Similar inclusion geometries and effects have been observed in the isomorphous crystal structure of β-CD ethanol octahy-

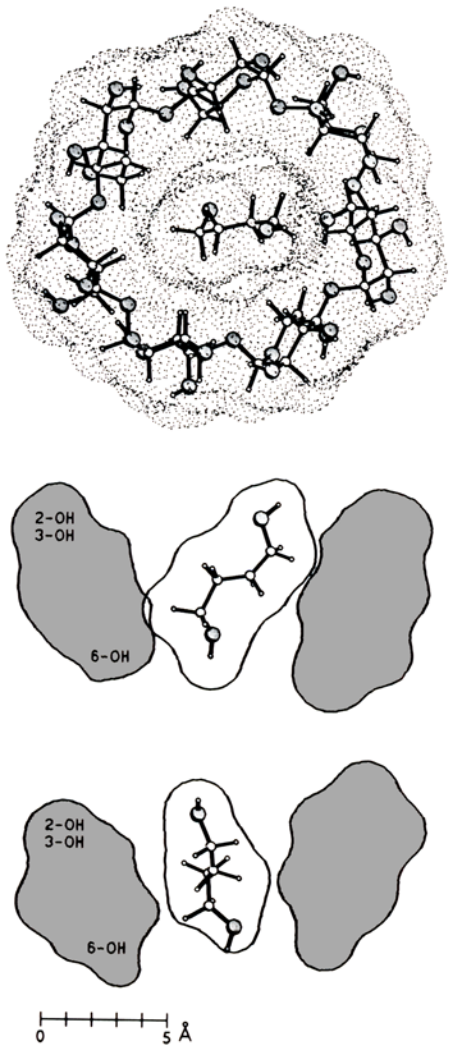

Figure 3. *Top:* Contact surface (in dotted form with ball-and-stick model insert) of the β-CD 1,4-buandediol · 6.25H_2O inclusion complex [40] with the water molecules left off. Due to the low atomic resolution of the structure determination for the vibrating chain ligand, only its mean atomic positions were taken into consideration. The mode of viewing onto the cyclodextrin macrocycle corresponds to Figure 1. – *Center and bottom:* Two mutually perpendicular surface cross-sections through the center of geometry of the complex, the loose steric fit displaying the extended conformational space available to the guest.

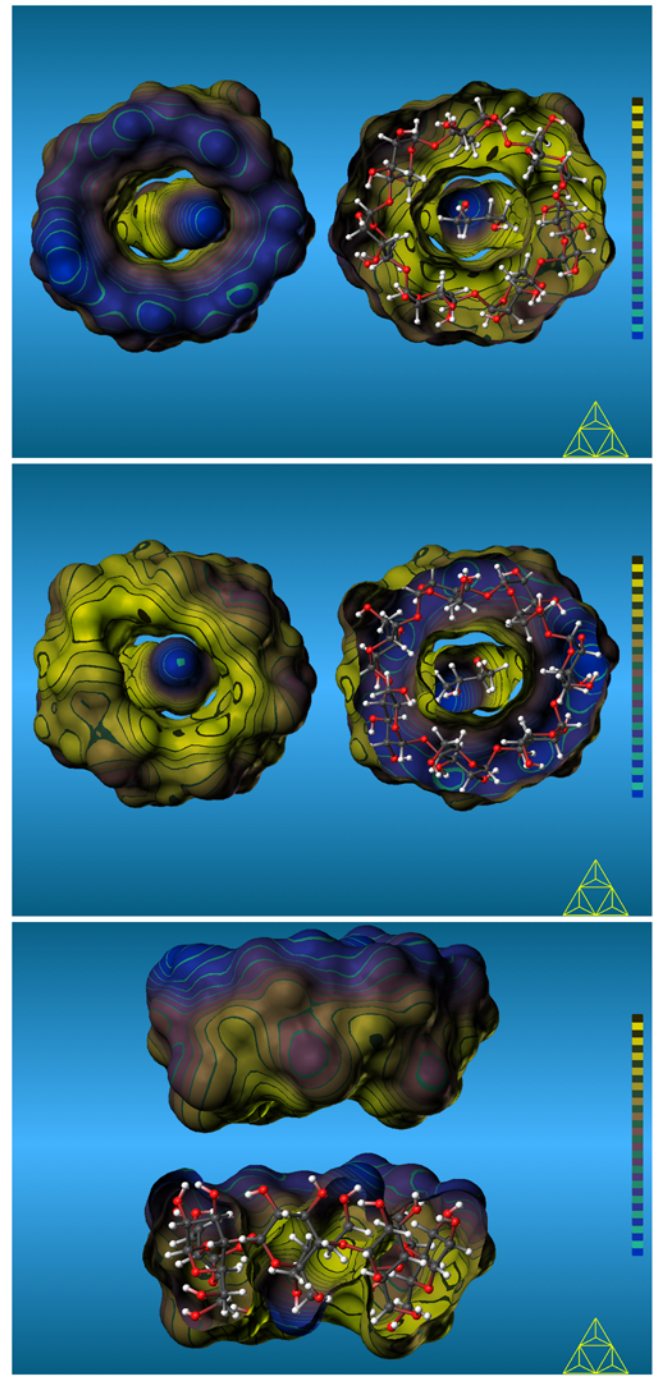

Figure 4. Representation of the hydrophobic characteristics (lipophilicity maps) of the β-CD 1,4-butanediol inclusion complex (mean atomic positions were used for the guest) [40] in the same color-code as in Figure 2. In all modelings, the color-scale was adapted individually to the range of values calculated separately for the guest and host. The *top* picture gives the front-side view onto the distinctively hydrophilic (blue), wide-opened 2-OH/3-OH aperture of the β-cyclodextrin, with the half-opened surface model juxtaposed to it. The *center* entry displays the back-side, i.e. the narrower 6-CH_2OH opening of the torus, in closed and bisected form each. – *Bottom:* The side-view models without and with surface clipping impressively illustrate the 1,4-butanediol guest molecule to fully penetrate the cavity of the host. Its most hydrophobic molecular regions (yellow) are matching the hydrophobic surface regions of the cavity in the cyclodextrin molecule and are fully masked by the host.

drate [41]: Ethanol – representing half the structural motif of 1,4-butanediol – is fixed by its hydroxyl group approximately in the plane described by all the 2-O and 3-O atoms, with the ethyl residue pointing into the cavity and exhibiting substantial thermal motions.

2.3 β-Cyclodextrin complexes with adamantane-1-carboxylic acid and -1-methanol

The vast diversity with which cyclodextrins can include guest molecules, revealing in turn the variable interplay of different forces and effects, is vividly articulated by the molecular architectures to which β-CD assembles with two closely related adamantane derivatives: adamantane-1-carboxylic acid [42] and the respective alcohol [43]. While their solvent-accessible (contact) surfaces (Figure 5, top entries) reveal a rather tight fit of the bulky admantane moieties into the essentially non-distorted, round-shaped β-CD cavity, their side view cross-section plots (Figure 5, bottom) disclose distinct differences.

In the *1-carboxylic acid* case, the guest is either fully immersed in the cavity with the hydrophilic head group located at the primary hydroxyl side, or only with its admantyl portion, yet there is no direct hydrogen bond between the carboxyl-oxygens and the primary β-CD-hydroxyl groups in either of the two crystallographically detectable species; interestingly, however, two units of the complex are "fused together" to head-to-head dimers (Figure 5, bottom left) through intense hydrogen bonding network between the secondary hydroxyl groups at the two β-CD-tori. The alltogether 30 water molecules, with which the dimeric complex crystallizes, are all on the outside – understandably, as there is no free space to even include a water molecule into the cavity interior.

These unique features are similarly borne out by the highly hydrophobic (yellow) adamantyl moieties fully immersed

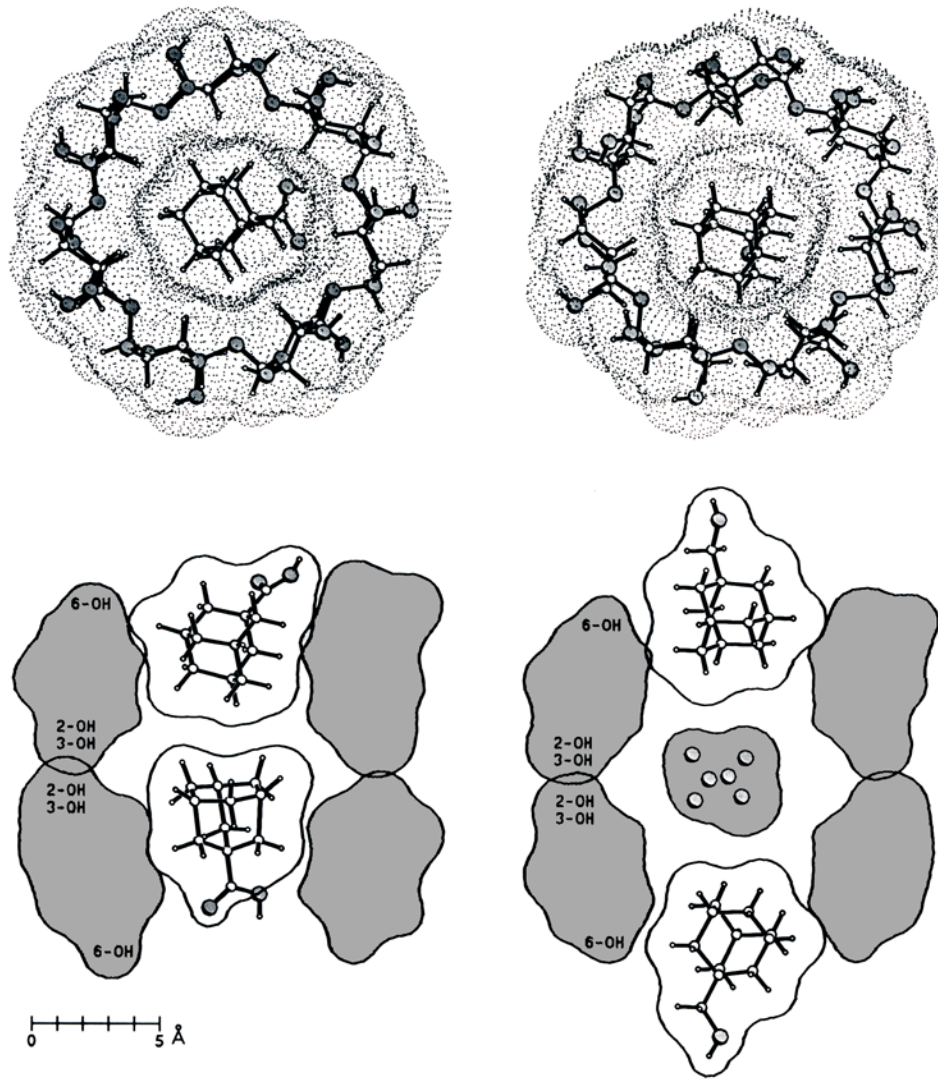

Figure 5. *Top:* Crystal structure derived molecular geometry and dotted contact surface of one unit each of the inclusion complexes of β-CD adamantane-carboxylic acid · $15H_2O$ [42] (*left*) and of β-CD admantane-methanol · $1.1H_2O$ [43] (*right*), viewed down from the secondary hydroxyl side (wider rim); the water molecules of crystallization are left off for clarity. – *Bottom:* Cross-section plots through the molecular surfaces of the respective dimers of these inclusion complexes as realized in the crystal lattice. In both cases, the secondary hydroxyl sides of two β-CDs are directed towards each other in a head-to-head arrangement, giving rise to a tightly bound dimer through an intense hydrogen bonding network. In the complexes, the adamantane-1-carboxylic acid (*left*) penetrates the cavity either fully (lower CD unit) or partially only (upper complex), each having the carboxyl group directed to the primary hydroxyl end of the CD host. The adamantane-methanol in the respective dimer (*bottom right*) protrudes from each of the narrower rim (6-CH_2OH side) in a symmetrical fashion. As indicated by the isolated shaded spheres, two water molecules are statistically disordered over six alternate crystallographic positions inside the cavity, occupying the empty space close to the interface of the two monomers.

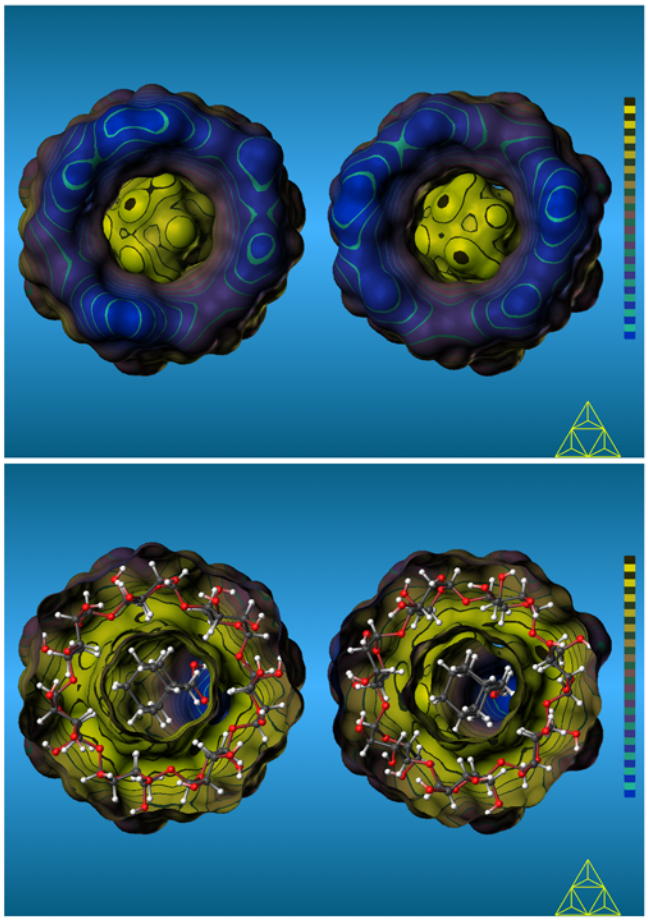

Figure 6. Molecular lipophilicity patterns (MLP's) of a monomeric unit each of the inclusion complexes β-CD adamantanecarboxylic acid [42] (*left*) and β-CD adamantane-methanol [43] (*right*), as realized in the solid state. The orientation of the complexes corresponds to that in Figure 5 (*top*), i.e. the 2-OH/3-OH face of the β-CD – distinctly hydrophilic (blue) in the *top* entry – uniformly facing the viewer. In the *bottom* images, the hydrophilic front halves have been removed, exposing a view onto the hydrophobic (yellow) primary hydroxyl side of the β-CD portions and the asymmetrically disposed adamantane moieties with their substituents (COOH *left*, CH_2OH *right*).

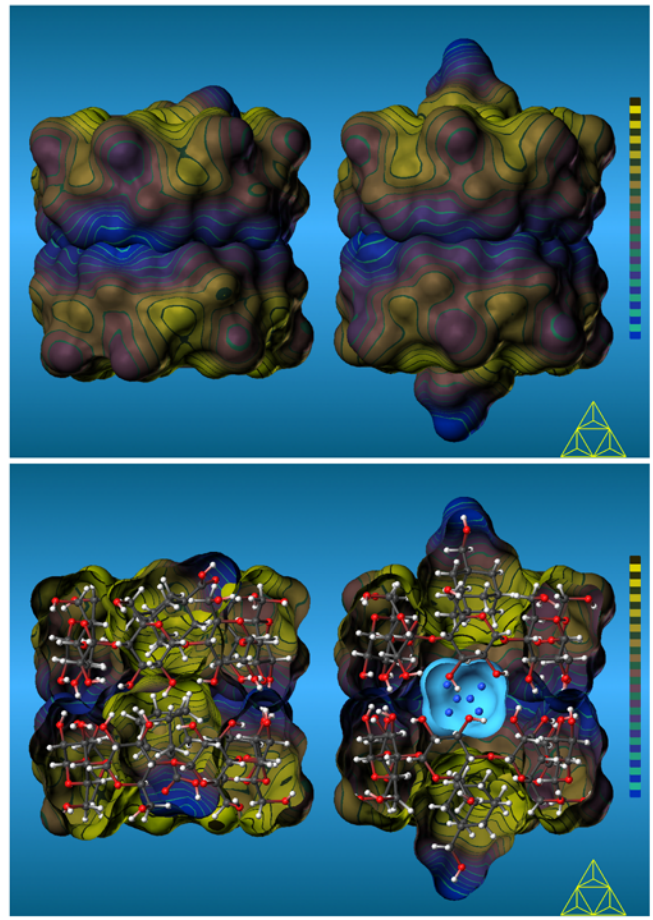

Figure 7. Side-view models representing the hydrophobic topographies (MLP's) of the dimeric units of the β-CD inclusion complexes with adamantane-1-carboxylic acid (*let* side each) and the respective 1-methanol (*right*); molecular orientation cf. Figure 5 (*bottom*). The solid surface models (*top* picture) and their bisected forms (*bottom* representations) indicate the tight interaction of the monomers at their most hydrophilic surface parts via an intense hydrogen bonding network between the 2-OH and 3-OH hydroxyl groups. The 30 water molecules outside the carboxylic acid dimer are omitted for clarity, while in the methanol analog the six crystallographic positions inside the cavity over which two different water molecules are distributed, are indicated by blue spheres. The light-blue surface displays the approximate steric volume demanded by these water molecules without indicating any surface quality or hydrophilic property. Aside the matching relationship between hydrophilic and hydrophobic surface areas in the guest and host, the major orienting factors for the respective overall assemblies seems to derive from the need to solvate the polar groups of the guest. Remaining empty space in a hydrophilic environment is filled with water in the crystal lattice.

into the dimer's cavity-inside, facing each other just as the tightly interlocked secondary hydroxyl sides of the two β-CD's do, generating thereby an intensely hydrophilic (blue) circular band around the equator of the dimer. The most hydrophobic (yellow) regions of the "double host" extend from this equator plane towards both ends which are determined by the hydrophilic carboxyl groups of the guest. This environment provides for the carboxyl group an dideal disposition to engage in hydrogen bonding to the CD-hydroxyl groups of the next dimer, or to water.

In the *adamantane-1-methanol* case [43] (Figure 5–7, right entries), the molecular architecture of the complex in the lattice is also characterized by a β-CD head-to-head dimer held together by extensive hydrogen bonding across the secondary hydroxyl sides, yet the "fusion" is less intense than in the carboxylic acid case. The major part of the adamantane moiety is located towards the other smaller opening (6-CH_2OH-face), from which parts of the hydrocarbon and the hydroxyl group stick out, thereby allowing the latter to engage in hydrogen bonding with a primary hydroxyl of an adjacent β-CD. The most interesting feature – and as such a distinct contrast to the carboxylic acid analog – is the water trapped at the dimer interface (two molecules per dimer), obviously preventing the secondary hydroxyl sides of the two β-CD's to come into closer contact.

The respective lipophilic patterns generated onto solvent-accessible surfaces (Figure 6 and 7, right entries) reflect this unique assembly of β-CD, guest, and water in such a way, that invariably an optimum match of hydrophobic and hydrophilic surface regions is reached between the three components: the central hydrophilic band formed by the "fused" β-CD's secondary hydroxyl sides wraps around the water encapsulated, the complementarity between hydrophobic adamantyl surface portions and hydrophobic CD-cavity areas is fully materialized, whereas the guest hydroxymethyl group protuding from either side of the dimer cavity is distinctly hydrophilic (blue).

In comparatively appraising the similarities and differences of the two complex assemblies, it appears obvious that the orientation of the two adamantane derivatives in the β-CD cavity as well as the association of the monomeric units to dimers, is primarily governed by the need to solvate the polar hydrophilic group of the guest – in the solid state by water of crystallization and/or hydroxyl groups of adjacent CD's, in aqueous solution by water molecules, very likely entailing the dissociation of the dimers. Accordingly, the hydrophobic interactions are deemed to play a secondary role, fine-tuning the orientation of the guest within the cavity to optimize corresponding of hydrophilic and hydrophobic surface regions.

2.4 The γ-cyclodextrin inclusion of a 12-crown-4 ether

As compared to its smaller ring homologs, relatively few crystal structures have been reported for γ-CD and its complexes. All of these are of high symmetry and indicate, that the γ-CD may well be the least distorted and at least strained of the cyclodextrins.

The inclusion complexes of γ-CD with the 12-crown-4 ether [44], partially in combination with various inorganic salts [45], clearly show the guest-host geometry relationship on a good atomic resolution, all structures being isomorphous with each other. Three crystallographically independent CD molecules A-B-C are stacked along a C_4-symmetry axis in a head-to-tail (A-B), head-to-head (B-C), and tail-to-tail (C-A) relationship, each enclosing a 12-crown-4 moiety with an approximately all-(-)*gauche* arrangement of the four consecutive -O-CH_2-CH_2-O-ring units (torsion angles $\approx -93^{\circ}$). In Figure 8, the molecular geometry of the salt-free γ-CD·12-crown-4 ether complex is shown in combination with its dotted contact surface. The CD torus is highly symmetrical with narrow variations of the glucose tilt angles ($<\tau> \approx 104^{\circ}$) and diagonal distances between interglycosidic oxygens of 11.75Å; also, the *Cremer-Pople* parameters indicate very little puckering, i.e. an essentially planar γ-CD macrocycle.

In addition, the cross section plot through the surface (Figure 8, bottom) illustrates the crown ether moiety to be included from the secondary hydroxyl side, i.e. the wide torus opening. The essentially perfect steric fit of the crown ether, sitting on the bulge ring in the cavity center originating from the 5-hydrogen and the interglycosidic oxygens, evokes the picture of a lid on the inner edge of a cone. The solid surface models provided in Figure 9 emphasize this nearly flawless "lock-and-key"-situation even more lucidly.

The lipophilicity profiles generated in the usual way [27, 29] and projected onto the contact surfaces in color-coded form [30] (Figure 9), attest to the impressive conformity of the most hydrophobic and most hydrophilic surface regions at the guest-host interface – despite of the obvious fact, that the two compounds differ significantly in their absolute hydrophobicities. The polar-apolar side differentiation of the crown ether moiety is caused by the spatial separation of its four ring oxygens and eight methylene units pointing towards opposite directions, thus contributing to opposite surface regions. The hydrophobic methylene groupings are directed into the inner part of the hydrophobic cavity, while the polar oxygen atoms are located close to the hydrophilic torus rim made up by the secondary glucose hydroxyls.

The location of all ether oxygens on the same side causes a shallow surface dent at the center of the crown ether (cf. side-views in Figure 9), which is amenable for interactions with cations. Indeed, in the γ-CD·12-crown-4 complexes with co-crystallized inorganic salts, the cations are located in a double-decker fashion between the center of two head-to-head arranged γ-CD units, with the crown ethers providing a suitable environment for eight-fold coordination for the metal ion [45]. An analogous coordination is not possible between head-to-head and head-to-tail stacked CD pairs, entailing that only two third of the crown ether units in one-third of the CD layers interact with a cation; the other remain "empty".

3 Conclusion

The far-reaching or complete coonformity between hydrophobic and hydrophilic surface regions of various guests and the cavities of α-CD, β-CD and γ-CD, emerging from the computer-generated lipophilicity patterns described above, provide ample evidence for the importance of the reciprocal interplay of such interactions.

Remains the question, to which extent lipophilic interactions between host and guest are inducing forces for the complex formation, are determining the orientation of the guest in the cavity, and contribute to the stability of the complex. It is obvious that, at the present state of our knowledge, this question cannot be answered, as the "hydrophobic effect" – even if one has agreed on the exact definition of the term [22] – can neither be quantified reliably, nor can it be separated from the various other factors involved in the complex formation, such as dipole-dipole alignments and compensation of entropic and enthalpic parameters associated with solvation changes in the guest and host. All of these interactions are in-

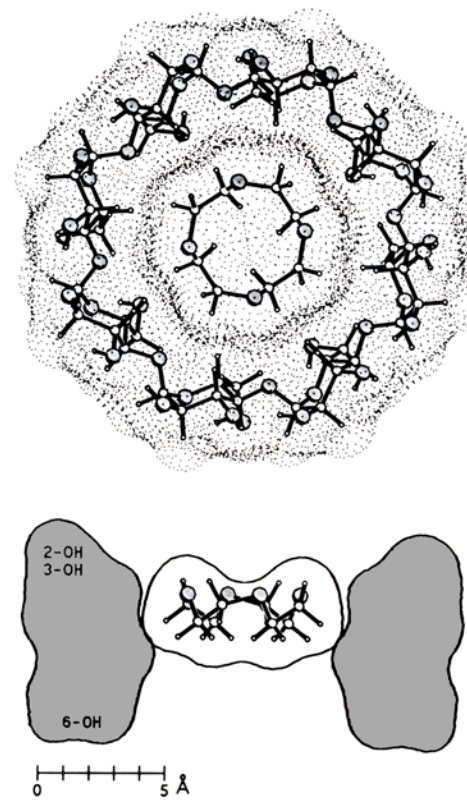

Figure 8. *Top:* Geometry and dotted contact surface of one γ-CD · 12-crown-4 ether unit in the salt-free solid-state structure of the nonahydrate [44]; the water of crystallization was removed for clarity. The *bottom* model corresponds to the surface intersection with a plane perpendicular to the cyclodextrin ring and through the geometrical center of the complex, clearly exposing the lid-like, asymmetric inclusion of the crown ether guest by the γ-cyclodextrin host; the mode of viewing of the CD corresponds to Figure 1 and 3.

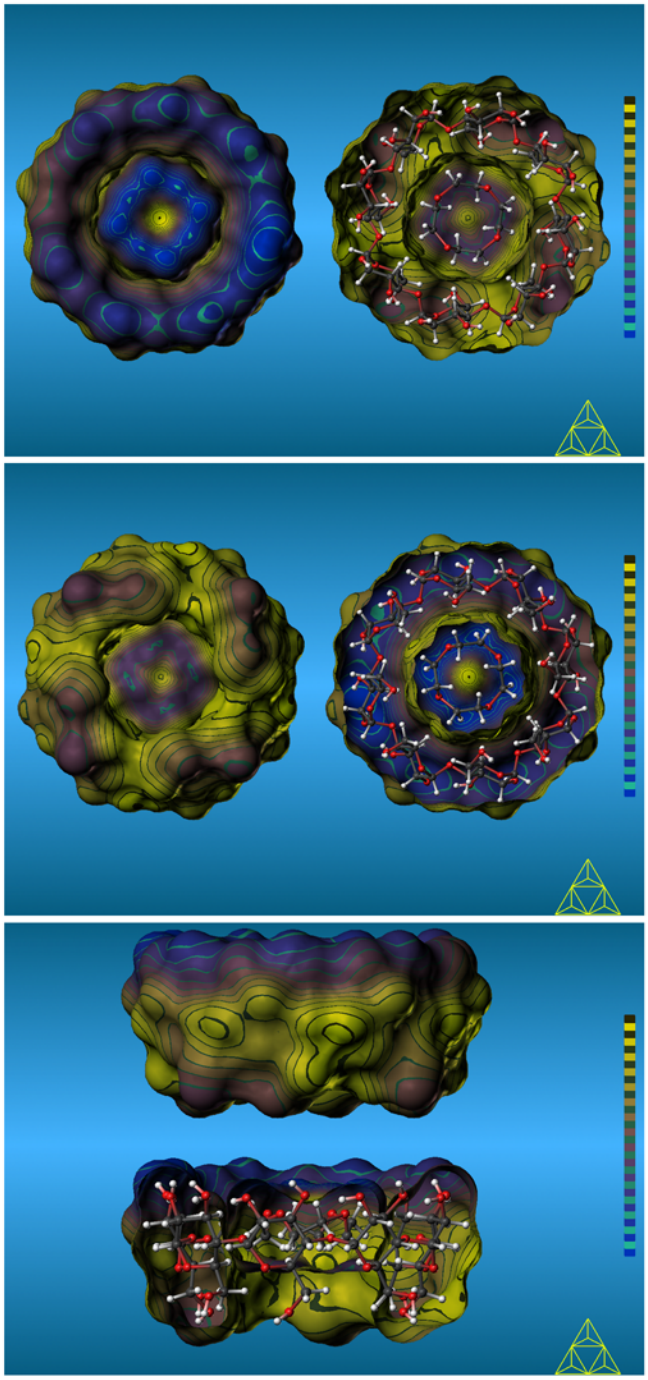

Figure 9. Hydrophobic topography (MLP) of one structural subunit of the γ-CD 12-crown-4 inclusion complex [44]; the color-code applied, the mode of scaling, and the molecular orientations shown are analogous to Figure 2 and 4. The side-view models again illustrate the alignment of hydrophobic and hydrophilic molecular regions on the interface between the host and the crown ether guest molecule, the latter being asymmetrically diposed towards to the larger 2-OH/3-O opening of the cyclodextrin.

terconnected and obviously can enhance themselves in a cooperative way such that the overall effect is significantly greater than the sum of the individual contributions.

That the induced-fit theory [20] is closer to reality than the rigid key-lock concept [21] has been unequivocally established for a large number of enzymes [46] and, accordingly, may be inferred to apply to all cyclodextrins in the same way. This means that the inclusion complex formation of the cyclodextrins is not to be visualized as the insertion of a sterically fitting "key" into a matching "lock", but as a dynamic process with the reciprocal adaption of guest and CD-host towards each other. As this multifaceted process obviously requires the interplay and outbalancing of various different forces, whose relative proportions are exceedingly difficult to assess experimentally, it may well be that, at present, only advanced computational methodologies can provide the tools with which to tackle and eventually fully understand the complex formation of the cyclodextrins. The computation and visualization of hydrophobic and hydrophilic surface domains described in this account, and the substantiation of the complementarity of these domains at the guest/CD-host interface appears to be an essential contribution towards understanding formation and stability of cyclodextrin inclusion complexes.

4 Experimental

Molecular structures: All cyclodextrin geometries were obtained from the Cambridge Crystallographic Data File (CCDF) [47]: α-CD *p*-iodoaniline trihydrate ($C_{36}H_{60}O_{30} \cdot C_6H_6IN \cdot 3H_2O$, CCDF-Refcode: CDEXIA01) [34b], β-CD 1,4-butanediol · $6.25H_2O$ inclusion complex ($C_{42}H_{70}O_{35} \cdot C_4H_{10}O_2 \cdot 6.25H_2O$, KUTZKOZ) [40], β-CD 1-adamantane-carboxylic acid pentadecahydrate ($C_{42}H_{70}O_{35} \cdot C_{11}H_{16}O_2 \cdot 15H_2O$, BOGCAB) [42], β-CD 1-hydroxymethyl-adamantane undecahydrate ($C_{42}H_{70}O_{35} \cdot C_{11}H_{18}O_1 \cdot 11H_2O$, FASXUS) [43], and γ-CD · 12-crown-4 · $9H_2O$ ($C_{48}H_{80}O_{40} \cdot C_8H_{16}O_4 \cdot 9H_2O$, DOCYID) [44]. The water of crystallization has been removed in all cases, except for the hydroxymethyl-adamantane complex were the six water-oxygen positions (relative occupancies ≈0.33 each) inside the cavity of the dimeric unit are indicated in Figures 5 and 7. Hydrogen atoms not included in the determination of the crystal and molecular structures were positioned geometrically with standard bond lengths $r_{C\text{-}H} \approx 1.08$Å and $r_{O\text{-}H} \approx 0.90$Å, taking special care of possible intramolecular hydrogen bonding between neighboring hydroxyl groups. All molecular parameters discussed within this study have been re-calculated from this data set.

Molecular surfaces and molecular lipophilicity patterns (MLP's): Calculation of the molecular contact surfaces [28] and MLP's [29] was carried out by using the MOLCAD [27] molecular modelling program. Throughout, all surfaces and MLP's were calculated for separated molecules only, which were subsequently re-assembled to the monomeric and dimeric complexes. Color-coded projection of the MLP's onto the corresponding surfaces was done by applying texture mapping strategies [30]. Scaling of the hydrophobicity profiles was performed in arbitrary units and in relative terms for each molecule separately if not stated otherwise, and no absolute values are displayed. Color graphics were photographed from the computer screen of a SILICON-GRAPHICS workstation.

Acknowledgement

The authors are most grateful to Prof. Dr. *J. Brickmann,* Institut für Physikalische Chemie, Technische Hochschule Darmstadt, for generously providing us his MOLCAD modelling software package [27] and his sophisticated computational facilities.

Bibliography

[1] This account is *Part 11* of the series "Molecular Modelling of Saccharides". – Part 10: *Immel, S.,* and *F. W. Lichtenthaler:* Mo-

lecular electrostatic and lipophilic potential profiles of α-cyclofructin. Liebigs Ann. Chem. (1996), 39–44.
[2] For an authoratitive monograph see: *Bender, M. L.,* and *M. Komiyama:* Cyclodextrin Chemistry. Springer, Berlin 1978.
[3] *Saenger, W.:* Structural aspects of cyclodextrins and their inclusion complexes. Inclusion Compounds (J. L. Atwood, J. E. D. Davies, D. D. MacNicol, Eds.), Acad. Press, London, Vol. **2** (1984), pp. 231–259.
[4] *Clarke, R. J., J. H. Coates,* and *S. F. Lincoln:* Inclusion complexes of the cyclodextrins. Adv. Carbohydr. Chem. Biochem. **46** (1988), 205–249.
[5] [5a] *Szejtli, J.:* Cyclodextrin Technology. Kluver Acad. Publ., Dordrecht, NL, 1988.
[5b] *Szejtli, J.:* Medical applications of cyclodextrins. Med. Res. Rev. **14** (1994), 353–386.
[6] *Schurig, V.,* and *H. P. Novotny:* Gaschromatographic separation of enantiomers on cyclodextrin derivatives. Angew. Chem. **102** (1990), 969–986; Angew. Chem. Int. Ed. Engl. **29** (1990), 939–958.
[7] *Li, S.,* and *W. C. Purdy:* Cyclodextrins and their applications in analytical chemistry. Chem. Rev. **92** (1992), 1457–1470.
[8] *Wenz, G.:* Cyclodextrins as building blocks for supramolecular structures and functional units. Angew. Chem. **106** (1994) 851–870; Angew. Chem. Int. Ed. Engl. **33** (1994), 803–822.
[9] *Takahashi, K.,* and *K. Hattori:* Asymmetric reactions with cyclodextrins. J. Incl. Phenom. **17** (1994), 1–24.
[10] *Tabushi, I.:* Design synthesis of artificial enzymes. Tetrahedron **40** (1984), 269–292.
[11] *Cully, J., H. R. Vollbrecht,* and *J. Wiesmüller:* Removal of cholesterol from egg yolk. German Offenl. DE 3,928,258 (1991); Chem. Abstr. **114** (1991), 205800e.
[12] *Harata, K.:* Recent advances in the X-ray analysis of cyclodextrin complexes. Inclusion Compounds (J. L. Atwood, J. E. D. Davies, D. D. MacNicol, Eds.), Oxford Univ. Press, Oxford, UK, Vol. **5** (1991), pp. 311–344.
[13] *Inoue, Y.:* NMR studies of the structure and properties of cyclodextrins and their inclusion complexes. Annual Reports NMR Spectrosc. **27** (1993), 59–101.
[14] [14a] *Koehler, J. E. H., W. Saenger,* and *W. F. van Gunsteren:* A molecular dynamics simulation of crystalline α-CD hexahydrate. Eur. Biophys. **15** (1987), 197–210.
[14b] *Koehler, J. E. H., W. Saenger,* and *W. F. van Gunsteren:* Conformational differences between α-CD in aqueous solution and in crystalline form. J. Mol. biol. **203** (1988), 241–250.
[14c] *Koehler, J. E. H., W. Saenger,* and *W. F. van Gunsteren:* On the occurence of three-center hydrogen bonds in cyclodextrins in crystalline form and in aqueous solution. J. Biomol. Struc. Dyn. **6** (1988), 182–198.
[14d] *Koehler, J. E. H., W. Saenger,* and *W. F. van Gunsteren:* MD simulation of crystalline β-CD dodecahydrate at 293 and 120K. Eur. Biophys. J. **15** (1987), 211–224.
[14e] *Koehler, J. E. H., W. Saenger,* and *W. F. van Gunsteren:* The flip-flop hydrogen bonding phenomenon. MD simulation of crystalline β-CD. Eur. Biophys. J. **16** (1988), 153–168.
[15] *Lipkowitz, K. B.:* Symmetry breaking in cyclodextrins. A molecular mechanics investigation. J. Org. Chem. **56** (1991), 6357–6367.
[16] *Bakó, I.,* and *L. Jicsinszky:* Semiempirical calculations on cyclodextrins. J. Inclusion Phenom. Mol. Recogn. Chem. **18** (1994), 275–289.
[17] *Mark, A. E., S. P. van Helden, P. E. Smith, L. H. M. Janssen,* and *W. F. van Gunsteren:* Convergence properties of free energy calculations. α-Cyclodextrin complexes as a case study. J. Am. Chem. Soc. **116** (1994), 6293–6302.
[18] *Dodziuk, H.,* and *K. Nowinski:* Structure of cyclodextrins and their complexes. Do cyclodextrins have a rigid truncated cone structure? J. Mol. Struc. (THEOCHEM) **110** (1994), 61–68.
[19] *Lichtenthaler, F. W.,* and *S. Immel:* On the hydrophobic characteristics of cyclodextrins: Computer-aided visualization of molecular lipophilicity patterns. Liebigs Ann. Chem. (1996), 27–37.
[20] *Koshland, D. E., Jr.:* The key-lock theory and the induced-fit theory. Angew. Chem. **106** (1994), 2368–2372; Angew. Chem. Int. Ed. Engl. **33** (1994), 2375–2378.
[21] *Lichtenthaler, F. W.:* 100 Years lock-and-key principle. What made *Emil Fischer* use this analogy? Angew. Chem. **106** (1994), 2456–2467; Angew. Chem. Int. Ed. Engl. **33** (1994), 2364–2374.
[22] *Blokzijl, W.,* and *J. B. F. N. Engberts:* Hydrophobic effects, opinions and facts. Angew. Chem. **105** (1993), 1610–1624; Angew. Chem. Int. Ed. Engl. **32** (1993), 1545–1579.
[23] *Lichtenthaler, F. W.,* and *S. Immel:* Sucrose, sucralose, and fructose. Correlations between hydrophobicity potential profiles and AH-B-X assignments. Sweet Taste Chemoreception (Eds.: M. Mathlouthi, J. A. Kanters, G. G. Birch), Elsevier Appl. Science, London/New York 1993, pp. 21–53.
[24] *Lichtenthaler, F. W.,* and *S. Immel:* Computer-simulation of chemical and biological properties of sucrose, the cyclodextrins, and of amylose. Internat. Sugar J. **97** (1995), 12–22.
[25] *Immel, S., J. Brickmann,* and *F. W. Lichtenthaler:* Small ring cyclodextrins: their geometries and hydrophobic topographies. Liebigs Ann. Chem. 1995, 929–942.
[26] *Lichtenthaler, F. W.,* and *S. Immel:* Cyclodextrins, cyclomannins, and cyclogalactins with five and six (1→4)-linked sugar units: Comparative assessment of their conformations and hydrophobicity potential profiles. Tetrahedron Asymmetry **5** (1994), 2045–2060.
[27] [27a] *Brickmann, J.:* MOLCAD – MOLecular Computer Aided Design, Technische Hochschule Darmstadt, 1992. The major part of the MOLCAD – program is included in the SYBYL package of TRIPOS Associates, St. Louis, USA.
[27b] *Brickmann, J.:* Molecular graphics – how to see a molecular scenario with the eyes of a molecule. J. Chim. Phys. **89** (1992), 1709–1721.
[27c] *M. Waldherr-Teschner, T. Goetze, W. Heiden, M. Knoblauch, H. Vollhardt,* and *J. Brickmann:* MOLCAD – Computer-aided visualization and manipulation of models in molecular science. Acvances in Scientific Visualization (Eds.: F. H. Post, A. J. S. Hin), Springer Verlag, Heidelberg, 1992, pp. 58–67.
[27d] *Brickmann, J., T. Goetze, W. Heiden, G. Moeckel, S. Reiling, H. Vollhardt,* and *C.-D. Zachmann:* Interactive visualization of molecular scenarios with MOLCAD/SYBYL, in Data Visualization in Molecular Science – Tools for Insight and Innovation (Ed.: J. E. Bowie), Addison-Wesley Publ., Reading, Mass., 1995, pp. 83–97.
[28] [28a] *Richards, F. M.:* Areas, volumes, packing, and protein structure. Ann. Rev. Biophys. Bioeng. **6** (1977), 151–176; Carlsberg. Res. Commun. **44** (1979), 47–63.
[28b] *Connolly, M. L.:* Analytical molecular surface calculation. J. Appl. Cryst. **16** (1983), 548–558; Science **221** (1983), 709–713.
[29] *Heiden, W., G. Moeckel,* and *J. Brickmann:* A new approach to analysis and display of local lipophilicity/hydrophilicity mapped on molecular surfaces (MLP). J. Comput.-Aided Mol. Des. **7** (1993), 503–514.
[30] *Teschner, M., C. Henn, H. Vollhardt, S. Reiling,* and *J. Brickmann:* Texture mapping, a new tool for molecular graphics. J. Mol. Graphics **12** (1994), 98–105.
[31] *Harata, K.:* Crystal structures of α-CD complexes with *p*-nitrophenol and *p*-hydroxybenzoic acid. Bull. Chem. Soc. Jpn. **50** (1977), 1416–1424.
[32] [32a] *Komiyama, M.,* and *H. Hirai:* ^{13}C NMR study on cyclodextrin inclusion complexes in solution. Bull. Chem. Soc. Jpn. **54** (1981), 828–831.
[32b] *Yamamoto, Y., M. Onda, M. Kitagawa, Y. Inoue,* and *Chûjô, R.:* NOE determination of qualitative host-guest relationships in α-CD inclusion complexes. Carbohydr. Res. **167** (1987), C11–C16.
[33] *Harata, K., H. Uedaira,* and *J. Tanaka:* The crystal structure of the α-CD *m*-nitrophenol (2:1) complex. Bull. Chem. Soc. Jpn. **51** (1978), 1627–1634.
[34] [34a] *Harata, K.:* The crystal and molecular structure of the α-CD*p*-iodoaniline complex. Bull. Chem. Soc. Jpn. **48** (1975), 2409–2413. –
[34b] *Saenger, W., K. Beyer,* and *P. C. Manor:* Topography of cyclodextrin inclusion complexes. The crystal structure of α-CD-*p*-iodoaniline trihydrate. Acta Crystallogr., Sect B **32** (1976), 120–128.

[35] For each glucose unit, the tilt angle τ denotes the inclination of the pyranose ring toward the macrocyclic ring perimeter, i.e. the angle between the cyclodextrin mean plane of all intersaccharidic (i.e. anomeric) oxygen atoms versus the least-squares best-fit mean plane through the six pyranoid ring atoms (C_1-C_2-C_3-C_4-C-O_5); for a graphical representation of this definition see ref. [19, 24].

[36] [36a] *Harata, K., K. Uekama, M. Otagiri, F. Hirayama,* and *H. Ogino:* Crystal structure of α-cyclodextrin-benzaldehyde (1:1) complex hexahydrate. Bull. Chem. Soc. Jpn. **54** (1981), 1954–1959.
[36b] *Harata, K.:* Crystal structure of the cyclohexaamylose *p*-iodophenol complex. Carbohydr. Res. **48** (1976), 265–270.
[36c] *Harata, K.:* The structure of the Cyclodextrin complex. XII. Crystal Structure of α-cyclodextrin1-phenylethanol (1:1) tetrahydrate. Bull. Chem. Soc. Jpn. **55** (1982), 1367–1371.
[36d] *Harata, K.:* Crystal Structure of the α-cyclodextrin-sodium benzene sulfonate complex. Bull. Chem. Soc. Jpn. **49** (1976), 2066–2072.
[36e] *Harata, K.:* Crystal structure of the α-cyclodextrinsodium 1-propanesulfonate nonahydrate. Bull. Chem. Soc. Jpn. **50** (1977), 1259–1266.

[37] *Harata, K.:* Crystal structures of α-CD complexes with 2-pyrrolidine and NN-dimethylformamide. Bull. Chem. Soc. Jpn. **52** (1979), 2451–2459.

[38] *Harata, K., K. Uekama, M. Otagiri,* and *F. Hirayama:* Crystal Structure of the αCD-3-iodopropionic acid (1:1) complex pentahydrate. Nippon Kagaku Kaishi 1983, 173–180; Chem. Abstr. **98** 135 604u.

[39] *Harata, K.:* Crystal structure of the inclusion complex of hexakis-(2,6-dimethyl)-α-CD with 3-iodopropionic acid. Carbohydr. Res. **192** (1989), 33–44.

[40] *Steiner, T., G. Koellner,* and *W. Saenger:* A vibrating flexible chain in a molecular cage; crystal structure of the complex β-CD-1,4-butanediol·6.25H_2O. Carbohydr. Res. **228** (1992), 321–332.

[41] *Steiner, T., S. A. Mason,* and *W. Saenger:* Cooperative OH···O hydrogen bonds in β-CD-ethanol octahydrate. J. Am. Chem. Soc. **112** (1990), 6184–6190; **113** (1991), 5676–5687.

[42] *Hamilton, J. B.,* and *M. N. Sabesan:* Structure of a complex of β-CD with 1-adamantanecarboxylic acid. Acta Crystallogr., Sect. **B 38** (1982), 3063–3069.

[43] *Hamilton, J. A.:* Crystal structure of the β-CD-adamantanemethanol inclusion complex Carbohydr. Res. **142** (1985), 21–37.

[44] *Kamitori, S., K. Hirotsu,* and *T. Higuchi:* Crystal and molecular structure of the γ-CD – 12-crown-4 (1:1) inclusion complex. J. Chem. Soc., Chem. Commun. 1986, 690–691.

[45] *Kamitori, S., K. Hirotsu,* and *T. Higuchi:* Crystal structures of double macrocyclic inclusion complexes composed of cyclodextrins, crown ethers, and cations. J. Am. Chem. Soc. **109** (1987), 2409–2414; Bull. Chem. Soc. Jpn. **61** (1988), 3825–3830.

[46] *Gerstein, M.; A. M. Lesk,* and *C. Chothia:* Structural mechanisms for domain movements in proteins. Biochemistry **33** (1994), 6739–6749.

[47] Cambridge Crystallographic Data File, Version 5.09 (1995). – *Allen, F. H., S. A. Bellard, M. D. Brice, B. A. Cartwright, A. Doubleday, H. Higgs, T. Hummelink, G. B. Hummelink-Peters, O. Kennard, W. D. S. Motherwell, J. R. Rodgers,* and *D. G. Watson:* The Cambridge Crystallographic Data Centre: Computer-based search, retrieval, analysis and display of information. Acta Crystallogr., Sect. **B 35** (1979), 2331–2339.

Addresses of authors: Professor Dr. Dr. h.c. *F. W. Lichtenthaler,* Dr. *S. Immel.* Technische Hochschule Darmstadt. Institut für Organische Chemie, Petersenstr. 22, D-64287 Darmstadt (Germany).

(Received: December 11, 1995).